Dynamics of the Binuclear Center of the Quinol Oxidase from *Acidianus ambivalens*†

Anna Aagaard,‡ Gwen Gilderson,‡ Cláudio M. Gomes,§ Miguel Teixeira,§ and Peter Brzezinski*,‡,||

Department of Biochemistry and Biophysics, Göteborg University, Medicinaregatan 9C, P.O. Box 462, SE-405 30 Göteborg, Sweden, Department of Biochemistry, The Arrhenius Laboratories for Natural Sciences, Stockholm University, SE-106 91 Stockholm, Sweden, and Instituto de Tecnologia Química e Biológica, Universidade Nova de Lisboa, Rua da Quinta Grande, 6, Apartado 127, 2780 Oeiras, Portugal

Received March 1, 1999; Revised Manuscript Received May 24, 1999

ABSTRACT: We have investigated the kinetic and thermodynamic properties of carbon monoxide binding to the fully reduced quinol oxidase (cytochrome aa_3) from the hyperthermophilic archaeon *Acidianus ambivalens*. After flash photolysis of CO from heme a_3, the complex recombines with an apparent rate constant of $\sim 3\ s^{-1}$, which is much slower than with the bovine cytochrome *c* oxidase ($\sim 80\ s^{-1}$). Investigation of the CO-recombination rate as a function of the CO concentration shows that the rate saturates at high CO concentrations, which indicates that CO must bind transiently to Cu_B before binding to heme a_3. With the *A. ambivalens* enzyme the rate reached 50% of its maximum level (which reflects the dissociation constant of the Cu_B(CO) complex) at $\sim 13\ \mu M$ CO, which is a concentration $\sim 10^3$ times smaller than for the bovine enzyme (~ 11 mM). After CO dissociation we observed a rapid absorbance relaxation with a rate constant of $\sim 1.4 \times 10^4\ s^{-1}$, tentatively ascribed to a heme-pocket relaxation associated with release of CO after transient binding to Cu_B. The equilibrium constant for CO transfer from Cu_B to heme a_3 was $\sim 10^4$ times smaller for the *A. ambivalens* than for the bovine enzyme. The $\sim 10^3$ times smaller Cu_B(CO) dissociation constant, in combination with the $\sim 10^4$ times smaller equilibrium constant for the internal CO transfer, results in an apparent dissociation constant of the heme a_3(CO) complex which is "only" about 10 times larger for the *A. ambivalens* ($\sim 4 \times 10^{-3}$ mM) than for the bovine (0.3×10^{-3} mM) enzyme. In summary, the results show that while the basic mechanism of CO binding to the binuclear center is similar in the *A. ambivalens* and bovine (and *R. sphaeroides*) enzymes, the heme-pocket dynamics of the two enzymes are dramatically different, which is discussed in terms of the different structural details of the *A. ambivalens* quinol oxidase and adaptation to different living conditions.

The hyperthermoacidophilic crenarchaeon *Acidianus ambivalens* is a member of the *Sulfolobales* that grows optimally at ∼80 °C and pH 2.5 (*1*, *2*). When grown aerobically using colloidal sulfur as an electron source, it expresses a very simple membrane-bound respiratory system, having A-type hemes as the major chromophores. It is constituted by a succinate dehydrogenase with a novel iron−sulfur clusters composition (*3*) that feeds electrons into a pool of caldariella quinone, a quinone specific of the *Sulfolobales*. This quinone then donates electrons to the only terminal oxidase present, a quinol oxidase (cytochrome aa_3), to which all membrane bound hemes are associated (*4*, *5*). The gene locci encoding for this oxidase contains five open reading frames (*6*). The enzyme is purified with four subunits, the largest of which has a molecular mass of 65 kDa (product of the *doxB* gene) and contains the ligands bound to the redox-active cofactors heme *a*, heme a_3, and Cu_B[1] (*6*). Thus, it is analogous to subunit I of the mitochondrial cytochrome *c* oxidase, although its homology is very low (14% identity, 32% similarity). Subunit II is totally dissimilar from most of the others known and as all quinol oxidases lacks any metal-binding motifs. Thus, the purified *A. ambivalens* enzyme contains three redox-active metal sites, heme *a* and a binuclear center consisting of heme a_3 and Cu_B (*4*, *5*). It has been postulated that caldariella quinone, the physiological electron donor, is in vivo tightly bound to the enzyme, providing the fourth redox active center (*5*).

High-resolution structures of cytochrome *c* oxidase from bovine heart (*7*−*9*) and *Paracoccus denitrificans* (*10*, *11*) have been determined. As was found previously from mutagenesis studies (*12*), they show that, in the binuclear center, Cu_B has three histidine ligands and the heme a_3 iron has a (proximal) histidine as an axial ligand. At the distal heme a_3 side, ligands such as O_2 and CO bind.

† Supported by grants to P.B. from the Swedish Natural Science Research Council and The Swedish Foundation for International Cooperation in Research and Higher Education (STINT) and to M.T. from Praxis XXI (BIO1075/94 and 36/97) and the European Union G-Project on Biotechnology of Extremophiles (Bio-4-CT96-0488).

‡ Göteborg University.
§ Universidade Nova de Lisboa.
|| Stockholm University.

[1] Abbreviations and definitions: Cu_B, copper B; τ, time constant (in $\exp(-t/\tau)$), i.e., a rate constant, $k = 1/\tau$; k_{Ba} and k_{aB}, rate constants for CO transfer from Cu_B to heme a_3 and from heme a_3 to Cu_B, respectively; $K_{Ba} = k_{Ba}/k_{aB}$, equilibrium constant; k_{on}, second-order CO-binding constant to Cu_B; k_{off}, CO dissociation from Cu_B; K_{CO}^{-1}, dissociation constant of the heme Cu_B(CO) complex; K_d, dissociation constant of the heme a_3(CO) complex; E_0, enzyme concentration; [X], concentration of X in units of mol/L; $[CO]_0$ and [CO] concentrations of added and free CO, respectively. If $E_0 \ll [CO]_0$, then $[CO]_0 = [CO]$.

10.1021/bi990473m CCC: $18.00
Published on Web 07/16/1999

In the functionally well-characterized membrane-bound bovine and *Rhodobacter sphaeroides* cytochrome *c* oxidase the catalytic reaction involves electron transfer from a water-soluble cytochrome *c* to a dinuclear Cu_A site, bound in subunit II, followed by consecutive intramolecular electron transfer to a low-spin heme *a* and to the binuclear center heme a_3-Cu_B, where oxygen binds and is reduced to water. The electron current from cytochrome *c* to O_2, through the enzyme, drives pumping of protons across the membrane (for a review see e.g. ref *13*).

Quinol oxidases lack the Cu_A site and electrons enter from the quinol, which binds to the enzyme (*14*). In the ubiquinol oxidase (cytochrome bo_3) from *E. coli*, the ubiquinol-binding site is likely to be found at the interface of subunits I and II (*15*). In this enzyme electrons are donated from ubiquinol to the low-spin heme *b* (cf. heme *a* in the bovine enzyme) and then to the oxygen-reducing binuclear center heme o_3-Cu_B (*16*, *17*).

The reaction of several cytochrome *c* and quinol oxidases with O_2 has been investigated in detail using various spectroscopic techniques. However, it is difficult to study the binding dynamics of the O_2 ligand to the reduced enzyme because the enzyme is oxidized and the first partly reduced oxygen intermediate is formed very rapidly after binding of O_2 to the binuclear center (within $\sim$50 μs in the bovine and *R. sphaeroides* enzymes (*18*)). In addition to O_2, the reduced binuclear center also binds other ligands such as carbon monoxide. Even though CO is not a natural ligand to cytochrome *c* oxidase, it can serve as a tool for investigation of the dynamic properties of the binuclear center. The CO−heme a_3 bond is photolabile, and thus, the complex can be photolyzed. Under anaerobic conditions, following flash-induced dissociation of CO from the reduced enzyme the ligand rebinds again to heme a_3. Thus after a short laser flash, both the CO-dissociation and -recombination kinetics can be investigated. In the bovine cytochrome *c* oxidase such investigations have provided abundant information on the structure and dynamics of the binuclear center and also of protein conformational changes coupled to ligand binding and dissociation (*19*−*23*). These types of investigations have attracted additional attention recently as it is thought that the proton-pumping machinery could be closely associated with the binuclear center and may involve changes in the coordination of metal ligands (*24*−*26*).

In this work we have investigated the CO-dissociation and -recombination kinetics in the quinol oxidase from *A. ambivalens*. The results are compared to those obtained from studies of the *R. sphaeroides* cytochrome *c* oxidase as well as to those obtained previously from studies of cytochrome *c* oxidase from bovine heart and from the thermophilic bacterium *Thermus thermophilus* (cytochrome ba_3). In the bovine enzyme, after flash-induced dissociation of CO from reduced heme a_3, CO binds transiently to Cu_B in a few picoseconds, after which it dissociates and equilibrates with the bulk solution with a rate constant of about $\sim 5 \times 10^5$ s^{-1} (*22*, *23*, *27*). The subsequent rebinding of CO to heme a_3 takes place through Cu_B. The transient binding of the ligand to Cu_B "on the way" to heme a_3 is not unique to CO but has also been suggested for O_2 (*28*, *29*). Thus investigation of the thermodynamics and kinetics of the CO reaction is also important for understanding the reaction of the enzyme with O_2.

The data show that the CO-binding properties differ dramatically between the *A. ambivalens* and bovine (and *R. sphaeroides*) enzymes. In the *A. ambivalens* enzyme, after flash photolysis of CO from the fully reduced enzyme, CO recombines with a rate constant of $\sim$3 s^{-1}, i.e., $\sim$25 times slower than with the bovine enzyme. The CO-recombination kinetics saturates to 50% at about 13 μM and 16 mM for the *A. ambivalens* and *R. sphaeroides* enzymes (11 mM for the bovine enzyme (*22*)), which reflects transient binding of CO to Cu_B during CO recombination with heme a_3 and shows that formation of the $Cu_B(CO)$ complex saturates at $\sim 10^3$ times lower concentration for the *A. ambivalens* enzyme than for the *R. sphaeroides* enzyme. In addition, the results indicate that the transfer of CO from Cu_B to heme a_3 is $\sim 10^3$ times slower in the *A. ambivalens* than in the *R. sphaeroides* and bovine enzymes.

MATERIALS AND METHODS

Cell Growth and Enzyme Purification. A. ambivalens (DSM 3772) cells were grown as described in ref *30*, and the quinol oxidase was purified as previously described (*5*). The protein concentration was determined using the pyridine hemochrome method (*31*). The enzyme concentration was verified from the reduced-minus-oxidized difference spectrum using an absorption coefficient of 23.2 mM^{-1} cm^{-1} at 605 nm (*32*).

Kinetic Measurements of CO Dissociation and Recombination. The enzyme stock solution was washed on a PD-10 column (Pharmacia) to replace the 400 mM potassium phosphate (pH 6.5), 0.1% dodecyl-β-D-maltoside buffer, in which the stock solution was stored, by 50 mM potassium phosphate at pH 7.8, 0.1% dodecyl-β-D-maltoside. The enzyme solution was transferred to a modified anaerobic cuvette, the concentration was adjusted to about 2−10 μM (depending on experiment; see figure legends), phenazine methosulfate (PMS) was added at a concentration of 5 μM, and the mixture was then repeatedly evacuated on a vacuum line and flushed with N_2. To reduce the enzyme, sodium ascorbate at 2 mM was added to the enzyme solution, followed by replacement of N_2 by CO. The concentration of enzyme with CO bound to heme a_3 was estimated from the absorbance difference spectrum reduced CO minus reduced using $\Delta\epsilon^{445} = 67$ mM^{-1} cm^{-1} (*33*). The fraction of the heme $a_3^{2+}(CO)$ complex was found to be about 60%, which did not change with temperature in the range 10−50 °C.

Direct Measurements of Thermal CO-Dissociation Kinetics. The solution of the reduced cytochrome *c* oxidase−CO complex was transferred anaerobically to one of the drive syringes of a locally modified stopped-flow apparatus (Applied Photophysics, DX-17MV). The other syringe was filled with the same buffer solution supplemented with 0.05% dodecyl-β-D-maltoside, equilibrated with air. The enzyme: air-equilibrated-solution mixing ratio was 1:1, giving an O_2 concentration in the experiment (after mixing) of 125 μM. The temperature of the samples in the syringes and the cuvette was controlled by a flow of anaerobic, thermostated water.

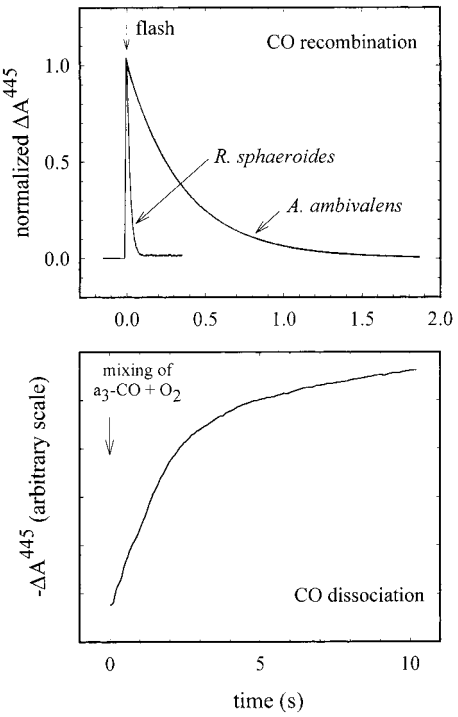

FIGURE 1: (A) Flash-induced absorbance changes associated with dissociation and recombination of CO from *A. ambivalens* quinol oxidase and *R. sphaeroides* cytochrome *c* oxidase. (B) Absorbance changes associated with reaction of the fully reduced *A. ambivalens* quinol oxidase with O_2. A solution of the ascorbate-reduced enzyme was mixed with an air-equilibrated buffer solution in a stopped-flow apparatus at $t = 0$. The (irreversible) reaction rate of the reduced enzyme with O_2 is assumed to be limited by the CO-dissociation rate from heme a_3 ($k_{aB} \cong 1.2 \pm 0.2$ s^{-1}). The absorbance difference corresponds to the difference in absorbance of the reduced enzyme−CO complex and the oxidized enzyme. Experimental conditions: (A, B) 2 μM enzyme, 50 mM potassium phosphate, pH 7.8, 0.1% dodecyl-β-D-maltoside, 1 mM CO, 22 ± 1 °C; (A) 2 mM sodium ascorbate, 1 mM CO; (B) after mixing with a mixing ratio of 1:1 1 mM sodium ascorbate, 0.5 mM CO, 125 μM O_2.

The laser and observation equipment have been described in detail elsewhere (*18*).

Measurements of the CO-Recombination Kinetics and Extent of CO Binding to Heme a_3 as a Function of CO Concentration. A 3-mL four-window fluorescence cuvette was filled with an enzyme solution, and the cuvette was closed using a rubber septum. Care was exercised to avoid trapping of air between the liquid and the rubber septum. Excess dithionite was added to reduce the enzyme, which was confirmed from an absorption spectrum in the range 400−700 nm. Aliquots of a CO-saturated buffer solution containing 1 mM CO and ∼1 mM dithionite were added to the enzyme solution. After each addition, flash-induced absorbance changes at 445 nm were recorded.

For measurements at CO concentrations >1 mM a locally designed pressure cell was used. The CO pressure was varied in the range 0.1−5 MPa.

RESULTS

Recombination of CO with the Fully Reduced Enzyme after Flash Photolysis. Figure 1 shows absorbance changes at 445 nm after pulsed illumination of the fully reduced-CO complex of the quinol oxidase (cytochrome aa_3) from *Acidianus ambivalens*. The initial increase in absorbance is associated with dissociation of CO. It is followed by a slower decrease in absorbance, associated with recombination of CO with the fully reduced enzyme. At 1 mM the CO-recombination absorbance change displayed a single recombination phase with a rate of 3.0 ± 0.2 s^{-1}, which is about 25 times slower than with the bovine cytochrome aa_3 at the same CO concentration (∼80 s^{-1}). The CO-recombination rate was the same at pH 5 and 9 as well as for the enzyme in the native membranes (data not shown).

Thermal CO Dissociation from the Fully Reduced Enzyme. The dissociation rate of CO from heme a_3^{2+} was measured by mixing the fully reduced-CO complex of the enzyme with an O_2-containing solution in a stopped-flow apparatus. Dioxygen binds rapidly and irreversibly to the reduced enzyme (because O_2 is trapped by rapid oxidation of the enzyme;
$\tau \cong 100$ μs; Gilderson et al., unpublished results). Therefore, the oxidation rate of the enzyme is limited by the CO-off rate. Upon mixing of the reduced-CO complex with O_2, biphasic kinetics was observed at 445 nm. Since we assume that CO must dissociate before any reaction can take place after mixing of the enzyme and O_2 solutions, the faster of the two phases was taken as being associated with dissociation of CO from heme a_3. Its rate was found to be 1.2 ± 0.2 s^{-1} at 22 °C. This rate is similar to that found with the *T. thermophilus* cytochrome ba_3 (0.8 s^{-1} (*34*)), but it is about 50 times slower than that found with the bovine enzyme (0.023 s^{-1} (*35*)).

CO-Recombination Characteristics as a Function of CO Concentration. The CO-recombination characteristics were investigated at different CO concentrations in the range 0.25 μM to 1 mM. Figure 2A shows the CO-recombination rate as a function of the CO concentration for the *A. ambivalens* quinol oxidase and *R. sphaeroides* cytochrome *c* oxidase. As seen in Figure 2A, with both the quinol and cytochrome *c* oxidases, the rate does not increase linearly with CO concentration, as has been found with myoglobin, but the CO-recombination rate saturates at high CO concentrations, as has been found with the bovine cytochrome *c* oxidase. However, the CO concentration at which the rate saturates is $\sim 10^3$ times smaller for the *A. ambivalens* enzyme than for the *R. sphaeroides*, bovine (*22*) and *E. coli* enzymes (*36*; see also ref *37*). The saturation behavior has previously been attributed to transient binding of CO to Cu_B prior to intramolecular transfer of CO from Cu_B to heme a_3 (see Discussion).

Figure 2B shows the amplitude of the kinetic phase associated with CO recombination for the *A. ambivalens* quinol oxidase. This amplitude reflects the enzyme fraction with CO bound to heme a_3^{2+}. For the *A. ambivalens* enzyme a dissociation constant of $(4 \pm 1) \times 10^{-3}$ mM was determined, as compared to 0.3×10^{-3} mM for the bovine enzyme (*35*, *50*).

Rapid, CO-Concentration-Independent Absorbance Changes after CO Dissociation. When measured on a shorter time scale, a faster component was observed after dissociation of CO from the fully reduced enzyme (Figure 3). It displayed a rate constant of $(1.4 \pm 0.5) \times 10^4$ s^{-1}. Upon addition of Stigmatellin, an inhibitor which presumably binds to (and blocks) the quinone-binding site, the rate of the μs-absorbance change was slower and displayed a rate constant of $(6 \pm 2) \times 10^3$ s^{-1} (not shown).

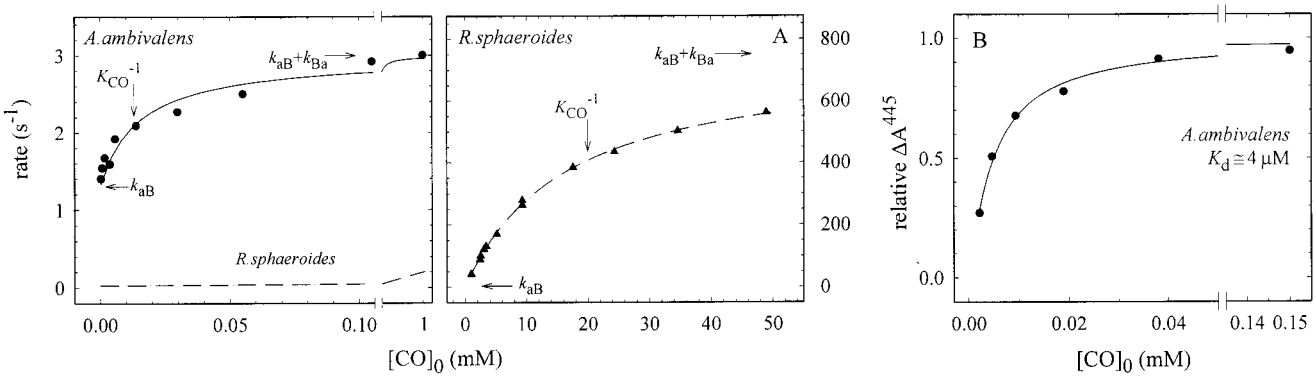

FIGURE 2: (A) Apparent CO-recombination rate (k_{obs}, see eq A2) as a function of the CO concentration of added CO ([CO]$_0$) in the *A. ambivalens* quinol oxidase and *R. sphaeroides* cytochrome *c* oxidase. The lines represent a fit of eq A2 with the data (cf. the parameters indicated in the graph). (B) Amplitude of the flash-induced CO dissociation absorbance change at 445 nm as a function of CO concentration. The line represents a fit of eq A5 with the data (cf. the parameters indicated in the graph). Experimental conditions were the same as those in Figure 1A, except that the CO concentration was varied as indicated.

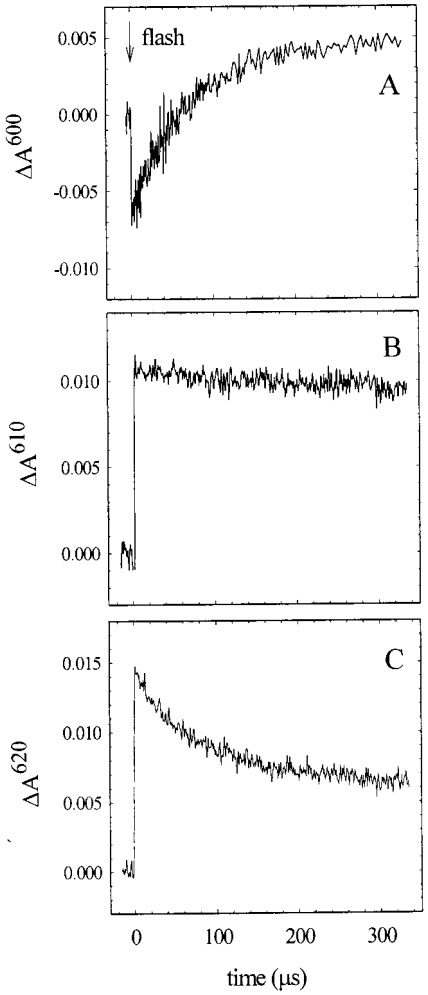

FIGURE 3: The μs-phase following flash-induced CO dissociation from the *A. ambivalens* quinol oxidase at (A) 600 nm, (B) 610 nm, and (C) 620 nm. Experimental conditions were the same as those in Figure 1A.

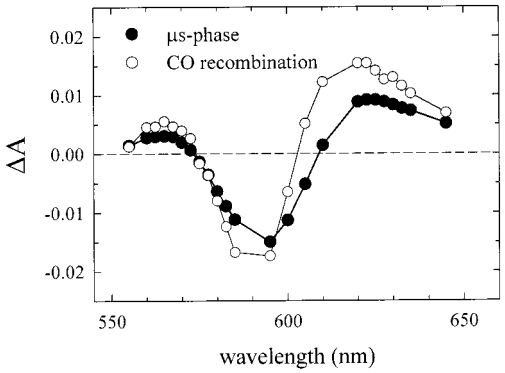

FIGURE 4: Kinetic difference spectra of the CO recombination (○) and the μs relaxation (●) absorbance changes. Experimental conditions were the same as those in Figure 1A.

The kinetic difference spectrum (Figure 4) of the μs-relaxation was different from that of the CO recombination. In addition, the rate of the μs-relaxation was independent of CO concentration, which shows that the μs-relaxation is not associated with rapid CO recombination.

Temperature Dependence of Events Associated with CO Dissociation and Recombination. Figure 5 shows the temperature dependence of the CO-dissociation and -recombination rates (k_{aB} and k_{obs}; see Discussion and Appendix), as well as the rapid absorbance relaxation (μs relaxation) following CO dissociation in the range 3−45 °C. The CO-recombination experiments were done using a CO concentration of about 1 mM, i.e., in a range in which the recombination rate is independent of the CO concentration (cf. Figure 2). Consequently, we did not have to account for the change in CO concentration (dissolved CO) with temperature. The activation energies for the CO recombination, CO dissociation and for the μs-relaxation (not shown) were 66, 63, and 40 kJ·mol^{-1}, respectively. The solubilized enzyme was stable for at least 1 h at 50 °C. With the bovine enzyme the activation energy for CO dissociation from heme a_3 was ~90 kJ·mol^{-1} (data not shown), i.e., larger than with the *A. ambivalens* enzyme.

As indicated in Materials and Methods, at 22 °C about 60% of the enzyme population did bind CO. This fraction did not change with temperature in the range 10−50 °C, which is consistent with the temperature dependence of the equilibrium constant for CO transfer between heme a_3 and Cu_B (Figure 5; see Discussion).

Formation of the Mixed-Valence Enzyme. We also tried to investigate internal electron transfer in the *A. ambivalens* enzyme after flash photolysis of CO from the partially reduced enzyme (*38*). We were not able to observe any electron transfer, which reflects the very large difference in reduction potentials between the two hemes (*5*).

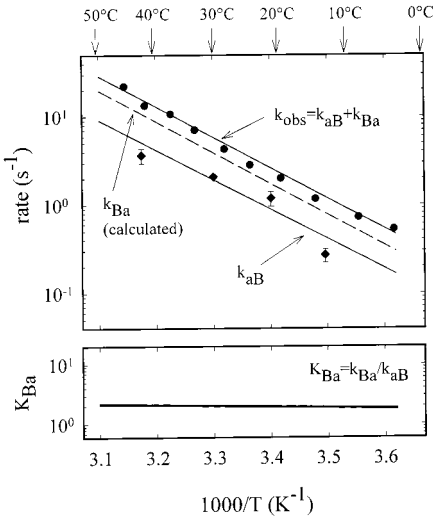

FIGURE 5: (A) Temperature dependence of CO-recombination (●) and CO-dissociation (◆) rates. The CO-recombination rate was measured at saturating CO concentrations, and thus, $k_{obs} = k_{aB} + k_{Ba}$. The CO-transfer rate from heme a_3 to Cu_B (CO-dissociation rate from heme a_3, k_{aB}) was measured after mixing of the fully reduced CO complex with an O_2 solution (see legend to Figure 1 and Materials and Methods). The CO-transfer rate in the opposite direction, i.e., from Cu_B to heme a_3 (k_{Ba}, dashed line), was calculated from a difference of the least-squares fits to k_{obs} and k_{aB}. Similarly, the equilibrium constant K_{Ba} was calculated from a ratio of k_{Ba} and k_{aB}. The temperature-independent K_{Ba} was confirmed from an independent spectrophotometric study of the fraction of the heme a_3(CO) complex formed as a function of temperature in the range 5−50 °C. Experimental conditions for measurements of k_{obs} and k_{aB} were the same as those in panels A and B, respectively, of Figure 1.

DISCUSSION

In this study we have investigated the kinetics of dissociation and recombination of the fully reduced-CO complex of the quinol oxidase (cytochrome aa_3) from *A. ambivalens*. Both the kinetic and thermodynamic properties of these reactions in the *A. ambivalens* quinol oxidase differ dramatically from those of cytochrome *c* oxidase from bovine heart (and *R. sphaeroides*).

The reactions following CO dissociation in the bovine enzyme have been investigated in detail using various time-resolved spectroscopic techniques. Alben et al. (*39*, *40*) showed that after flash-induced dissociation of CO from heme a_3 the ligand binds to Cu_B. At temperatures below ~140 K the CO ligand is trapped at Cu_B whereas at higher temperatures the binding is transient and is followed by equilibration of CO with the bulk solution. Woodruff et al. (*22*, *23*, *27*) investigated the kinetics of this reaction in detail and showed that after photolysis of the heme a_3−CO bond, CO binds to Cu_B within ~1 ps after which it dissociates and equilibrates with the bulk CO in ~1.5 μs. Most interestingly, absorbance changes in the visible range were observed on the same time scale as the release of CO from Cu_B. These absorbance changes were attributed to changes in the heme a_3 environment. Consequently, the possibility was discussed that a structural change in the heme pocket may be coupled to CO dissociation from Cu_B. This suggestion goes back to the original observation of Findsen et al. (*20*) who used time-resolved resonance Raman spectroscopy to show that immediately after flash photolysis of CO from heme a_3, the Fe−proximal His vibration initially has a higher frequency (~221 cm^{-1}) than that of the relaxed species (~215 cm^{-1}). The vibration relaxes to its equilibrium frequency with a time constant of ~1 μs; i.e., it coincides in time with the release of CO from Cu_B. Findsen et al. (*20*) suggested that, immediately after dissociation of CO from heme a_3, the heme pocket is in a different conformation from that in the fully reduced unligated enzyme. The heme pocket then relaxes to the equilibrium conformation in about 1 μs. Woodruff and co-workers (*22*, *23*) instead suggested that binding of CO to Cu_B and heme a_3 is controlled by an endogenous ligand. In the heme a_3(CO) complex this ligand is bound to Cu_B. Upon dissociation of CO from heme a_3 the ligand moves and binds to heme a_3 on the distal side, which allows binding of CO to Cu_B. At the same time the proximal histidine Fe_{a_3} bond is broken. The release of CO from Cu_B (τ = 1.5 μs) is accompanied by the ligand switching back from heme a_3 to the copper with re-formation of the proximal-histidine−Fe_{a_3} bond, a process which is responsible for the observed absorbance changes in the visible range.

In a recent study, on the basis of results from picosecond time-resolved resonance Raman experiments Babcock and co-workers (*19*) found that the proximal-histidine−Fe_{a_3} bond most likely remains intact after CO dissociation and proposed that the observed heme a_3 absorbance changes on the μs-time scale may be caused by a μs-relaxation of the proximal-histidine−Fe_{a_3} bond after dissociation of CO. Such a relaxation may be coupled to changes in the protein structure because of an increase in the out-of-plane distance of the heme a_3 iron (on the μs time scale) as a result of the CO dissociation (*19*).

Rebinding of CO to heme a_3 involves a transient binding to Cu_B, which is reflected by the saturation of the CO-recombination kinetics at sufficiently high CO concentrations (*22*, *36*). In other words, the CO from solution first equilibrates with Cu_B and is then "transferred" intramolecularly to heme a_3, where the intramolecular transfer rate determines the CO-recombination rates at saturating CO concentrations. This model is supported by studies of mutant enzymes in which histidine ligands of Cu_B in ubiquinol oxidase from *E. coli* were modified, which resulted in loss of Cu_B (*36*). In these mutant enzymes the CO-recombination kinetics did not saturate at high CO concentrations, but the rate increased linearly with increasing CO concentration, similarly to the behavior of myoglobin. The same behavior was observed with the corresponding mutants of the *R. sphaeroides* enzyme prepared in the laboratory of R. B. Gennis (Aagaard et al., unpublished data).

In the *A. ambivalens* quinol oxidase the CO-recombination rate displayed saturation behavior, which indicates that also in this enzyme CO binds transiently to Cu_B prior to binding to heme a_3 (after flash photolysis of heme a_3(CO) complex). After CO dissociation, a transient absorbance change with a time constants of ~70 μs was observed (without stigmatellin; see below). The kinetic difference spectrum of the μs-absorbance change was similar to the difference spectrum of the 1.5 μs change in the bovine enzyme (*22*), and we therefore tentatively ascribe the μs-events in the *A. ambivalens* quinol oxidase to a relaxation of the heme-a_3 pocket which is associated with the release of CO from Cu_B after transient binding following flash-induced dissociation from heme a_3.

Table 1: Rates and Equilibrium Constants for Reactions Associated with Dissociation and Recombination of CO with *Acidianus Ambivalens* Quinol Oxidase and Bovine Cytochrome *c* Oxidase

		A. ambivalens		
determined from	rate or equilib const	22 °C	37 °C	bovine 20 °C
O_2 reaction	k_{aB} (s^{-1})	1.2 ± 0.2	~3.7	0.023[b]
CO-recomb kinetics	k_{aB} (s^{-1})	1.1 ± 0.2		0.027[c]
	k_{Ba} (s^{-1})	1.9 ± 0.2	~6.9	1030[c]
	K_{Ba}	1.7 ± 0.5	~1.9	3.8×10^4 [c]
	K_{CO}^{-1} (mM)	$(13 \pm 4) \times 10^{-3}$	$\sim 22 \times 10^{-3}$ [a]	11[c]
	calcd $K_d = K_{CO}^{-1}/(1 + K_{Ba})$ (mM)	$(4.8 \pm 0.5) \times 10^{-3}$		
amplitude	K_d (mM)	$(4 \pm 1) \times 10^{-3}$	$6 \pm 1 \times 10^{-3}$	$\sim 0.3 \times 10^{-3}$ [d]
μs-phase rate (k_{off})	k_{off} (s^{-1})	$(1.4 \pm 0.5) \times 10^4$	$\sim 4.5 \times 10^4$	4.7×10^5 [c]
k_{off} and K_{CO} ($k_{on} = K_{CO} k_{off}$)	k_{on} (M^{-1} s^{-1})	$(1 \pm 0.8) \times 10^9$	$\sim 2 \times 10^9$	6.8×10^7 [c]

[a] Calculated from K_d and K_{Ba}, not from CO-recombination kinetics. [b] From refs *35* and *51*. [c] From ref *22*. [d] From refs *35* and *50*.

Scheme 1: Model for CO Binding to the Fully Reduced Binuclear Center of *Acidianus ambivalens* Quinol Oxidase and Cytochrome *c* Oxidase

$$Fe^{2+}_{a3}\ Cu^{+}_{B} + CO \underset{k_{off}}{\overset{k_{on}}{\rightleftharpoons}} Fe^{2+}_{a3}\ Cu^{+}_{B}(CO) \underset{k_{aB}}{\overset{k_{Ba}}{\rightleftharpoons}} Fe^{2+}_{a3}(CO)\ Cu^{+}_{B}$$

$$K_{CO} = k_{on}/k_{off} \qquad K_{Ba} = k_{Ba}/k_{aB}$$

With stigmatellin the μs-relaxation was slower (~170 μs). This is consistent with recent resonance Raman studies (Das, Gomes, Teixeira, and Rousseau, unpublished data) which show that the heme-pocket conformation changes upon binding of quinone.

Kinetic and Thermodynamic Parameters of CO Dissociation and Recombination. On the basis of the discussion above the reactions following dissociation of CO from the *A. ambivalens* quinol oxidase were modeled using the same model as for the bovine cytochrome *c* oxidase (Scheme 1). The rates constants were determined from the data in Figures 1−3, as described in the Appendix, and are summarized in Table 1.

The experimentally observed characteristics of the CO dissociation and recombination and the differences between the *A. ambivalens* and bovine enzymes are discussed below in terms of the model in Scheme 1.

CO-Recombination Kinetics (k_{obs}). The observed CO-recombination rate at 1 mM CO was about 20 times slower with the *A. ambivalens* (3 s^{-1}) than with the bovine heart (80 s^{-1}) and *R. sphaeroides* (50 s^{-1}) enzymes. According to the model in Scheme 1, the observed CO-recombination rate (see eq A2) is determined by the fraction of enzyme with CO bound to Cu_B (α in eq A2) times the CO-transfer rate from Cu_B to heme a_3 (k_{Ba}) plus the rate in the opposite direction (k_{aB}). The slower recombination kinetics with the *A. ambivalens* enzyme is due to the much smaller value of k_{Ba} (1.9 s^{-1}) in the quinol oxidase than in the cytochrome *c* oxidases from bovine heart and *R. sphaeroides* (~1000 s^{-1}). Note that at 1 mM CO, the CO-recombination kinetics is at the saturation level with the *A. ambivalens* enzyme, i.e., $k_{obs} = k_{Ba} + k_{aB}$ (see eq A3), while with the cytochrome *c* oxidases at the same CO concentration the rate is far from the saturation level.

CO-Off Rate from Heme a_3 (k_{aB}). The CO-off rate from heme a_3 (k_{aB}) was determined using two independent methods, either measured directly by mixing the enzyme−CO complex with O_2 or by extrapolating the k_{obs} to [CO] = 0 (see Figure 2A). Both methods gave about the same value of 1.2 s^{-1} in the *A. ambivalens* quinol oxidase, i.e., about 30 times faster than with the bovine enzyme (see Table 1) but similar to that found previously with *T. thermophilus* cytochrome ba_3 (0.8 s^{-1} (*34*)).

Transfer Rate of CO from Cu_B to Heme a_3 (k_{Ba}). The transfer rate of CO from Cu_B to heme a_3 (k_{Ba}) was determined from the CO-recombination rate (k_{obs}) at saturating CO concentrations ($k_{obs} \cong k_{aB} + k_{Ba}$) and k_{aB}. The rate constant was about a factor of 500 smaller in the *A. ambivalens* (1.9 ± 0.2 s^{-1}) than in the *R. sphaeroides* (750 ± 70 s^{-1}) and bovine (1030 s^{-1} (*22*, *23*)) enzymes.

Equilibrium Constant for CO Transfer between Heme a_3 and Cu_B (K_{Ba}). The rate constants for CO transfer from Cu_B to heme a_3 (k_{Ba}) and from heme a_3 to Cu_B (k_{aB}) were determined as described above. From the two rate constants, the equilibrium constant for transfer of CO from Cu_B to heme a_3 ($K_{Ba} = k_{Ba}/k_{aB}$) was determined to be 1.7 ± 0.5 in the *A. ambivalens* quinol oxidase, which is more that 10^4 times smaller than in the bovine enzyme (see Table 1).

CO-Recombination Rate as a Function of [CO]: Determination of the Dissociation Constant for Cu_B(CO) (K_{CO}^{-1}). While with the *A. ambivalens* enzyme the observed CO-recombination rate (k_{obs}) reached about 50% of the saturation level at 13 μM CO (K_{CO}^{-1}), the 50% level was reached at 16 mM CO with the *R. sphaeroides* enzymes (11 mM with the bovine enzyme (*22*)). As discussed above, according to Scheme 1 and eq A2 the observed recombination rate (k_{obs}) is the fraction CO bound to Cu_B (α) times the CO-transfer rate from Cu_B to heme a_3 (k_{Ba}) plus the rate in the opposite direction (k_{aB}), where $\alpha = [CO]/(K_{CO}^{-1} + [CO])$. Thus the different behavior observed with the *A. ambivalens* and bovine/*R. sphaeroides* enzymes, reflected in different α values, is due to the ~10^3 smaller dissociation constant (K_{CO}^{-1}) with the *A. ambivalens* than that with the bovine and *R. sphaeroides* enzymes.

Heme a_3(CO) Dissociation Constant. The dissociation constants for the heme a_3(CO) complex, K_d, was about a factor of 10−20 (cf. factor of ~80; in ref *5*) larger with the *A. ambivalens* than with the bovine/*R. sphaeroides* enzyme. According to the model in Scheme 1, $K_d = (K_{CO}(1 + K_{Ba}))^{-1}$ (see eq A5). Thus the relatively small difference in the K_d values, as compared to the difference in K_{CO}^{-1} and K_{Ba}, is due to the fact that K_d is essentially the ratio of the two and both are much smaller (by factors of ~10^3 and ~10^4, respectively) in the *A. ambivalens* than in the bovine/*R. sphaeroides* oxidases (see Table 1). This means that the smaller equilibrium constant K_{Ba} (i.e. less CO bound to heme a_3 as compared to Cu_B) in the *A. ambivalens* enzyme is

"compensated" by the larger fraction CO-bound Cu_B (larger α) in this enzyme.

CO-Recombination Rate at Low CO Concentrations. It is also interesting to note that at low CO concentrations eq A2 simplifies to the following:

$$k_{obs} \cong k_{aB} + k_{Ba}\frac{[CO]}{K_{CO}^{-1}} \quad [CO] \ll K_{CO}^{-1} \qquad (1)$$

The k_{Ba}/K_{CO}^{-1} values are 15×10^4 and 5×10^4 M^{-1} s^{-1} for the *A. ambivalens* and *R. sphaeroides* enzymes, respectively (9×10^4 M^{-1} s^{-1} for the bovine enzyme (*22*)), i.e., similar, which reflects the fact that at low CO concentrations the smaller k_{Ba} is "compensated" by the smaller K_{CO}^{-1} for the *A. ambivalens* enzyme. Thus, at low CO concentrations the dependence of k_{obs} on the CO concentration is similar.

Occupancy of the Heme a_3(CO) Complex. The value of the equilibrium constant for CO transfer between Cu_B and heme a_3, $K_{Ba} = k_{Ba}/k_{aB}$, of ~1.7 is consistent with the ~60% occupancy of the heme a_3(CO) complex in the fully-reduced enzyme. Since the temperature dependencies of the CO-transfer rates from heme a_3 to Cu_B (k_{aB}) and in the opposite direction (k_{Ba}) were about the same, the equilibrium constant is essentially independent of temperature (in the temperature range 3−45 °C). In other words, independently of the CO concentration and temperature (in the specified range) the heme a_3(CO) complex is formed in a maximum of ~60% of the enzyme population.

An occupation smaller than 100% for the heme a_3(CO) complex was also observed with the *T. thermophilus* cytochrome ba_3 (*34*, *41*), but in this case there was no obvious correlation with the K_{Ba} value.

Temperature Dependence of CO-Binding Characteristics. The rate of CO recombination in the *A. ambivalens* enzyme was measured as a function of temperature in the range 3−45 °C (see Figure 5). Since the experiments were done at a CO concentration of about 1 mM, the measured CO-recombination rate is at saturation and $k_{obs} \cong k_{aB} + k_{Ba}$. The temperature dependence of the CO-off rate from heme a_3 (k_{aB}) was measured by mixing the reduced enzyme−CO complex with an O_2-saturated solution at different temperatures. The Arrhenius activation energies of k_{obs} and k_{aB} were about the same (66 and 63 kJ·mol^{-1}, respectively). Consequently, the activation energy for the transfer of CO from Cu_B to heme a_3 (k_{Ba}) is ~65 kJ·mol^{-1}, as compared to ~45 kJ·mol^{-1} with the bovine enzyme (*22*).

It is interesting to note that extrapolation of CO-dissociation kinetics form Cu_B to ~80 °C gives a time constant which is similar to that of the bovine enzyme at ~20 °C (~1 μs).[2]

As indicated in the introduction, *Acidianus ambivalens* has an optimal growth temperature of about 80 °C. Due to instability of the *solubilized* enzyme we were not able to do experiments above 50 °C. However, extrapolation to 80 °C of the data obtained in the temperature ranges discussed above indicates that at 80 °C the rate and equilibrium constants discussed in this work for the *A. ambivalens* cytochrome aa_3 are still very different from those in the bovine enzyme, which may reflect adaptation to the living conditions of this archaeon.

The thermophilic enzymes have in general a low activity at mesophilic temperatures, which so far has been mainly attributed to a higher "rigidity" of the proteins at room temperatures (*42*, *43*); at the optimum growth temperature, the "rigidity" would be comparable to that of the mesophilic proteins (*42*, *43*). Recently, it has been proposed that the thermophilicity of the oxidases from *T. thermophilus* is a result of higher activation energies for the enzyme-catalyzed reactions (*34*). However, our data do not fully support this hypothesis. In fact, the activation energies for the processes discussed above for the archaeal oxidase are similar to those of the bovine one, and some are even lower for the *A. ambivalens* enzyme. Hence, clearly several different factors are involved in determining the overall kinetic behavior. In fact, it should be stressed that the *A. ambivalens* quinol oxidase and the *T. thermophilus* ba_3-type cytochrome *c* oxidase are among the most divergent oxidases of the heme−copper superfamily. Therefore, their unusual behavior may reflect adaptation strategies to high temperatures and low oxygen availability.

Functional Implications. Even though the transfer rates between Cu_B and heme a_3 and the dissociation constants are very different for CO and O_2 in cytochrome *c* oxidase, as indicated above, an investigation of the CO-binding properties reflects important functional differences between the *A. ambivalens* quinol oxidase and cytochrome *c* oxidase, which may provide information about the kinetic coupling of events (such as electron and proton transfer) associated with O_2 binding and reduction. In addition to differences in the dynamic features, the equilibrium constants K_{Ba} and K_{CO}^{-1} were 3−4 orders smaller in the *A. ambivalens* as compared to the bovine and *R. sphaeroides* enzymes. Since the dissociation constant of the heme a_3(CO) complex, K_d, is essentially the ratio of the two constants, the ratio of the K_d values in the *A. ambivalens* and bovine/*R. sphaeroides* enzymes is "only" about a factor of 10 (see Table 1). In other words, an unfavorable equilibrium constant for CO transfer from Cu_B to heme a_3 in *A. ambivalens* quinol oxidase is (partly) compensated by a large fraction of CO bound to Cu_B also at low CO concentrations.

It is interesting to note that many of the characteristic features of the *A. ambivalens* cytochrome aa_3 are shared with the *T. thermophilus* cytochrome ba_3, e.g., a slow CO recombination (k_{obs}), a slow transfer rate of CO from Cu_B to heme a_3 (k_{Ba}), a rapid dissociation of CO from heme a_3 (k_{aB}), and a small equilibrium constant for transfer of CO between Cu_B and heme a_3 (K_{Ba}) (*34*, *44*, *45*). Another common feature of the *A. ambivalens* cytochrome aa_3 and *T. thermophilus* cytochromes ba_3 and caa_3 is the extremely low CO concentration at which binding to Cu_B saturates (cf. K_{CO}^{-1} in Table 1, <100 and 250 μM for the *T. thermophilus* cytochromes ba_3 and caa_3, respectively (*44*)). Assuming the same qualitative behavior of O_2 as of CO binding, this high affinity of CO to Cu_B most likely reflects an adaptation to an environment with relatively low O_2 concentrations at which O_2 can be efficiently trapped by the enzyme (see ref *34*; cf. also ref *46*).

However, despite the similarities in the behaviors of the *A. ambivalens* and *T. thermophilus* oxidases, there are several

[2] The comparison only shows that the time constants are similar. To compare the function of the two enzymes under physiological conditions, data obtained with the bovine enzyme at ~37 °C should be used. Also time constants in the membrane-bound enzymes should be used.

key differences. While *A. ambivalens* is a thermoacidophilic archaea, *T. thermophilus* is a thermophilic bacterium and the amino-acid-sequence homology between the proteins is very low (~20%). Also, the archaeal enzyme is a caldariella quinol oxidase, while the *T. thermophilus* enzymes are cytochrome *c* oxidases. Furthermore, while the redox-potential difference between the low- and high-spin hemes in the *T. thermophilus* enzymes is similar to that of the bovine-heart enzyme, it is very different from that in the *A. ambivalens* quinol oxidase (*5*), suggesting that the environments of the hemes are different in the *T. thermophilus* and *A. ambivalens* enzymes. Interestingly, a similar difference between the redox potentials of the two hemes to that in the *A. ambivalens* enzyme was found in one of the terminal oxidases from *Sulfolobus* strain 7 (*47*).

As indicated above, dissociation of CO from heme a_3 results in a heme-pocket relaxation. The synchronous proximal-His relaxation and release of CO from Cu_B indicates that there is a coupling between ligand binding to Cu_B and the environment of heme a_3. In addition, structural data indicate that Cu_B may move upon binding of CO to heme a_3 (*7*). Moreover, recent time-resolved FTIR data (*24*, *25*) show that there is a link between events at the binuclear center and a protonatable amino-acid residue, glutamate-242 (in bovine cytochrome *c* oxidase) in subunit I, involved in proton transfer during the pumping steps of cytochrome *c* oxidase (reviewed in ref *48*). As pointed out by Babcock and colleagues (*49*), the transient ligand binding to Cu_B coupled to the heme-pocket relaxation and changes around amino-acid residues involved in proton pumping may reflect the fact that in cytochrome *c* oxidase the oxygen chemistry must be intimately coupled to proton transfer (pumping).

ACKNOWLEDGMENT

C.M.G. thanks the Programa Gulbenkian de Doutoramento em Biologia e Medicina and PRAXIS XXI (BD9793/96) for financial support. A.A., G.G., and P.B. are grateful to Mikael Oliveberg for help with design of the pressure cell used for CO-recombination experiments and to Lars Nordvall for continuous technical support.

APPENDIX: DETERMINATION OF THE RATE AND EQUILIBRIUM CONSTANTS FOR CO BINDING

Mechanistic Model. The model in Scheme 1 is assumed for binding of CO to the fully reduced enzyme (*22*). It is assumed that only one CO molecule can bind to the reduced binuclear center.

We assume that k_{on}, $k_{off} \gg k_{Ba}$, k_{aB}, a requirement that is fulfilled for both the *A. ambivalens* quinol oxidase and cytochrome *c* oxidase from *R. sphaeroides* and bovine heart (see below) at the CO concentrations used in this work.

Rate and Equilibrium Constants from Kinetic Data. The observed CO recombination rate (k_{obs}), i.e., the formation rate of the heme a_3(CO) complex after flash-induced dissociation of CO is

$$k_{obs} = k_{aB} + k_{Ba}\frac{k_{on}[CO]_0}{k_{off} + k_{on}[CO]_0} = k_{aB} + k_{Ba}\frac{[CO]_0}{K_{CO}^{-1} + [CO]_0} = k_{aB} + k_{Ba}\alpha \quad \text{(A2)}$$

where $[CO]_0$ is the concentration of added CO and $\alpha = [CO]_0/(K_{CO}^{-1} + [CO]_0)$ is the fraction enzyme in state $Fe_{a_3}^{2+}$-Cu_B^{+}(CO).

Equation A2 shows that the observed CO-recombination rate is the sum of the CO-off rate from heme a_3 (k_{aB}) and the on-rate (k_{Ba}) times the fraction enzyme with CO at Cu_B.

The dissociation rate of CO from heme a_3 (k_{aB}) can be determined by extrapolating k_{obs} to $[CO]_0 = 0$ in measurement of k_{obs} as a function of the CO concentration (see Figure 2). It was also determined independently from an experiment in which the enzyme−CO complex is mixed rapidly with an O_2-saturated solution (see Results), where the oxidation rate of the enzyme is determined by k_{aB}.

At saturating CO concentrations, i.e., $[CO]_0 \gg K_{CO}^{-1}$,

$$k_{obs} \cong k_{aB} + k_{Ba} \quad \text{(A3)}$$

Thus both k_{aB} and k_{Ba} can be determined experimentally.

Acidianus ambivalens Quinol Oxidase: A fit of eq A2 to the *A. ambivalens* quinol oxidase data in Figure 2 gives

$$k_{aB} = 1.1 \pm 0.2\ s^{-1} \quad k_{Ba} = 1.9 \pm 0.2\ s^{-1}$$
$$K_{Ba} = 1.7 \pm 0.5$$
$$K_{CO}^{-1} = (13 \pm 4) \times 10^{-6}\ M$$

at 22 °C.

Rhodobacter sphaeroides and Bovine Cytochrome *c* Oxidase: A fit of eq A2 to the *R. sphaeroides* cytochrome *c* oxidase data in Figure 2 gives

$$k_{aB} + k_{Ba} = 750 \pm 70\ s^{-1} \quad K_{CO}^{-1} = 16 \pm 2\ mM$$

at 22 °C, i.e., similar to those in the bovine enzyme (1030 s^{-1} and 11 mM, respectively (*22*)).

Since $k_{aB} \ll k_{Ba}$ and for CO concentrations above ~10 μM also $k_{aB} \ll \alpha k_{Ba}$, the k_{aB} term in eq A2 can be neglected. At CO concentrations below ~1 mM (corresponds to the CO concentration at 1 atm CO), eq A2 simplifies to

$$k_{obs} \cong k_{Ba}\frac{[CO]_0}{K_{CO}^{-1}} \cong 5 \times 10^4\ M^{-1}\ s^{-1}[CO]_0 \quad \text{(*R. sphaeroides* enzyme)}$$

i.e. the observed recombination rate increases linearly with increasing CO concentration with a second-order rate constant of $5 \times 10^4\ M^{-1}s^{-1}$, similar to that found with the bovine enzyme ($9 \times 10^4\ M^{-1}\ s^{-1}$ (*22*)).

Equilibrium Constants from Amplitude Data. The fraction enzyme with CO bound to heme a_3 was determined from the amplitude of the absorbance changes associated with CO recombination. Assuming the model in Scheme 1 and comparable CO and enzyme concentrations, the fraction of

enzyme in state $Fe_{a_3}^{2+}(CO)Cu_B^+$, χ, as a function of the concentration of added CO is

$$\chi([CO]_0) = \frac{K_{Ba}}{1+K_{Ba}} \frac{([CO]_0 + E_0 + K_d)}{2E_0} \times \left(1 - \sqrt{1 - \frac{4[CO]_0 E_0}{([CO]_0 + E_0 + K_d)^2}}\right) \quad \text{(A4)}$$

where $[CO]_0$ is the concentration of CO added to the enzyme solution, E_0 is the enzyme concentration, and K_d is the dissociation constant.

When $[CO]_0 \gg E_0$, the added CO concentration, $[CO]_0$, is approximately equal to the free CO concentration, [CO], and the fraction enzyme with CO bound to heme a_3 is

$$\chi([CO]) = \frac{K_{Ba}}{1+K_{Ba}} \frac{[CO]}{K_d + [CO]} \quad \text{(A5a)}$$

$$K_d = (K_{CO}(1+K_{Ba}))^{-1} \quad \text{(A5b)}$$

At saturating CO concentrations, i.e., $[CO] \gg K_d$, a limiting value for the fraction of the heme a_3(CO) complex formed is obtained:

$$\chi_{max} \cong \frac{K_{Ba}}{1+K_{Ba}} \qquad [CO] \gg K_d \quad \text{(A6)}$$

Maximum CO Binding to the A. ambivalens Quinol Oxidase. The equilibrium constant K_{Ba} is ~1.7 from which the maximum CO occupancy of the heme a_3 site, χ_{max}, can be determined using eq A6:

$$\chi_{max} \cong 0.6$$

The occupancy was also determined independently from the reduced-CO minus reduced difference spectrum and was found to be ~60% (see Materials and Methods and Results).

Determination of K_d for the A. ambivalens Quinol Oxidase. From a fit of eq A4 with the data in Figure 2B, the dissociation constant was determined at two different temperatures:

$$K_d = (4 \pm 1) \times 10^{-6}\ \text{M} \quad (22\ ^\circ\text{C})$$

$$K_d = (6 \pm 1) \times 10^{-6}\ \text{M} \quad (37\ ^\circ\text{C})$$

The approximate K_d value can also be calculated from the K_{CO} and K_{Ba} values, determined at 22 °C from the kinetics (see above), using eq A5b:

$$K_d = (K_{CO}(1+K_{Ba}))^{-1} \cong 13 \times 10^{-6}(1+1.7)^{-1}\ \text{M} \cong 4.8 \times 10^{-6}\ \text{M}$$

The K_d value at 37 °C is about a factor of 4 larger than that found from a CO titration of dithionite-reduced *A. ambivalens* quinol oxidase (*5*).

REFERENCES

1. Zillig, W., Yeats, S., Holz, I., Böck, A., Rettenberger, M., Gropp, F., and Simon, G. (1986) *Syst. Appl. Microbiol. 8*, 197−203.
2. Fuchs, T., Huber, H., Burggraf, S., and Stetter, K. O. (1996) *Syst. Appl. Microbiol. 19*, 56−60.
3. Gomes, C. M., Lemos, R. S., Teixeira, M., Kletzin, A., Huber, H., Stetter, K. O., Schäfer, G., and Anemüller, S. (1999) *Biochim. Biophys. Acta 1411*, 134−141.
4. Anemüller, S., Schmidt, C. L., Pacheco, I., Schäfer, G., and Teixeira, M. (1994) *FEMS Microbiol. Lett. 117*, 275−280.
5. Giuffrè, A., Gomes, C. M., Antonini, G., D'Itri, E., Teixeira, M., and Brunori, M. (1997) *Eur. J. Biochem. 250*, 383−388.
6. Purschke, W. G., Schmidt, C. L., Petersen, A., and Schafer, G. (1997) *J. Bacteriol. 179*, 1344−1353.
7. Yoshikawa, S., Shinzawa-Itoh, K., Nakashima, R., Yaono, R., Yamashita, E., Inoue, N., Yao, M., Fei, M. J., Libeu, C. P., Mizushima, T., Yamaguchi, H., Tomizaki, T., and Tsukihara, T. (1998) *Science 280*, 1723−1729.
8. Tsukihara, T., Aoyama, H., Yamashita, E., Tomizaki, T., Yamaguchi, H., Shinzawa-Itoh, K., Nakashima, R., Yaono, R., and Yoshikawa, S. (1996) *Science 272*, 1136−1144.
9. Tsukihara, T., Aoyama, H., Yamashita, E., Tomizaki, T., Yamaguchi, H., Shinzawa-Itoh, K., Nakashima, R., Yaono, R., and Yoshikawa, S. (1995) *Science 269*, 1069−1074.
10. Ostermeier, C., Harrenga, A., Ermler, U., and Michel, H. (1997) *Proc. Natl. Acad. Sci. U.S.A. 94*, 10547−10553.
11. Iwata, S., Ostermeier, C., Ludwig, B., and Michel, H. (1995) *Nature 376*, 660−669.
12. Calhoun, M. W., Thomas, J. W., Hill, J. J., Hosler, J. P., Shapleigh, J. P., Tecklenburg, M. M., Ferguson-Miller, S., Babcock, G. T., Alben, J. O., and Gennis, R. B. (1993) *Biochemistry 32*, 10905−10911.
13. Ferguson-Miller, S., and Babcock, G. T. (1996) *Chem. Rev. 96*, 2889−2907.
14. Trumpower, B. L., and Gennis, R. B. (1994) *Annu. Rev. Biochem. 63*, 675−716.
15. Tsatsos, P. H., Reynolds, K., Nickels, E. F., He, D. Y., Yu, C. A., and Gennis, R. B. (1998) *Biochemistry 37*, 9884−9888.
16. Svensson Ek, M., and Brzezinski, P. (1997) *Biochemistry 36*, 5425−5431.
17. Puustinen, A., Verkhovsky, M. I., Morgan, J. E., Belevich, N. P., and Wikström, M. (1996) *Proc. Natl. Acad. Sci. U.S.A. 93*, 1545−1548.
18. Ädelroth, P., Ek, M., and Brzezinski, P. (1998) *Biochim. Biophys. Acta 1367*, 107−117.
19. Schelvis, J. P. M., Deinum, G., Varotsis, C. A., Ferguson-Miller, S., and Babcock, G. T. (1997) *J. Am. Chem. Soc. 119*, 8409−8416.
20. Findsen, E. W., Centeno, J., Babcock, G. T., and Ondrias, M. R. (1987) *J. Am. Chem. Soc. 109*, 5367−5372.
21. Rousseau, D. L., Ching, Y., and Wang, J. (1993) *J. Bioenerg. Biomembr. 25*, 165−176.
22. Einarsdóttir, Ó., Dyer, R. B., Lemon, D. D., Killough, P. M., Hubig, S. M., Atherton, S. J., Lopez-Garriga, J. J., Palmer, G., and Woodruff, W. H. (1993) *Biochemistry 32*, 12013−12024.
23. Woodruff, W. H., Einarsdóttir, Ó., Dyer, R. B., Bagley, K. A., Palmer, G., Atherton, S. J., Goldbeck, R. A., Dawes, T. D., and Kliger, D. S. (1991) *Proc. Natl. Acad. Sci. U.S.A. 88*, 2588−2592.
24. Puustinen, A., Bailey, J. A., Dyer, R. B., Mecklenburg, S. L., Wikström, M., and Woodruff, W. H. (1997) *Biochemistry 36*, 13195−13200.
25. Hellwig, P., Behr, J., Ostermeier, C., Richter, O. M., Pfitzner, U., Odenwald, A., Ludwig, B., Michel, H., and Mäntele, W. (1998) *Biochemistry 37*, 7390−7399.
26. Morgan, J. E., Verkhovsky, M. I., and Wikström, M. (1994) *J. Bioenerg. Biomembr. 26*, 599−608.
27. Dyer, R. B., Einarsdóttir, Ó., Killough, P. M., Lopez-Garriga, J. J., and Woodruff, W. H. (1989) *J. Am. Chem. Soc. 111*, 7657−7659.

28. Oliveberg, M., and Malmström, B. G. (1992) *Biochemistry 31*, 3560−3563.
29. Blackmore, R. S., Greenwood, C., and Gibson, Q. H. (1991) *J. Biol. Chem. 266*, 19245−19249.
30. Teixeira, M., Batista, R., Campos, A. P., Gomes, C., Mendes, J., Pacheco, I., Anemüller, S., and Hagen, W. R. (1995) *Eur. J. Biochem. 227*, 322−327.
31. Berry, E. A., and Trumpower, B. L. (1987) *Anal. Biochem. 161*, 1−15.
32. Liao, G. L., and Palmer, G. (1996) *Biochim. Biophys. Acta 1274*, 109−111.
33. Vanneste, W. H. (1966) *Biochemistry 5*, 838−848.
34. Giuffrè, A., Forte, E., Antonini, G., D'Itri, E., Brunori, M., Soulimane, T., and Buse, G. (1999) *Biochemistry 38*, 1057−1065.
35. Gibson, Q. H., and Greenwood, C. (1963) *Biochem. J. 86*, 541−554.
36. Lemon, D. D., Calhoun, M. W., Gennis, R. B., and Woodruff, W. H. (1993) *Biochemistry 32*, 11953−11956.
37. Varotsis, C., Kreszowski, D. H., and Babcock, G. T. (1996) *Biospectroscopy 2*, 331−338.
38. Ädelroth, P., Sigurdson, H., Hallén, S., and Brzezinski, P. (1996) *Proc. Natl. Acad. Sci. U.S.A. 93*, 12292−12297.
39. Alben, J. O., Moh, P. P., Fiamingo, F. G., and Altschuld, R. A. (1981) *Proc. Natl. Acad. Sci. U.S.A. 78*, 234−237.
40. Fiamingo, F. G., Altschuld, R. A., Moh, P. P., and Alben, J. O. (1982) *J. Biol. Chem. 257*, 1639−1650.
41. Goldbeck, R. A., Einarsdóttir, Ó., Dawes, T. D., O'Connor, D. B., Surerus, K. K., Fee, J. A., and Kliger, D. S. (1992) *Biochemistry 31*, 9376−9387.
42. Vihinen, M. (1987) *Protein Eng. 1*, 477−480.
43. Jaenicke, R. (1991) *Eur. J. Biochem. 202*, 715−728.
44. Woodruff, W. H. (1993) *J. Bioenerg. Biomembr. 25*, 177−188.
45. Einarsdóttir, Ó., Killough, P. M., Fee, J. A., and Woodruff, W. H. (1989) *J. Biol. Chem. 264*, 2405−2408.
46. Verkhovsky, M. I., Morgan, J. E., Puustinen, A., and Wikström, M. (1996) *Nature 380*, 268−270.
47. Iwasaki, T., Matsuura, K., and Oshima, T. (1995) *J. Biol. Chem. 270*, 30881−30892.
48. Brzezinski, P., and Ädelroth, P. (1998) *J. Bioenerg. Biomembr. 30*, 99−107.
49. Babcock, G. T., Deinum, G., Hosler, J., Kim, Y., Pressler, M., Proshlyakov, D. A., Schelvis, J. P. M., Varotsis, C. A., and Ferguson-Miller, S. (1996) in *Oxygen Homeostasis and its Dynamics* (Ishimura, Y., Shimada, and Suematsu, M., Eds.), Vol. 1, pp 47−56.
50. Yoshikawa, S., Choc, M. G., O'Toole, M. C., and Caughey, W. S. (1977) *J. Biol. Chem. 252*, 5498−5508.
51. Greenwood, C., and Gibson, Q. H. (1967) *J. Biol. Chem. 242*, 1782−1787.

BI990473M